CATALOGED BY DDC
AS AD No. 424381

2-27-63-1 • AUGUST 1963

TECHNICAL REPORT

THE ABSORPTION COEFFICIENT OF NO_2

2-27-63-1

TECHNICAL REPORT

THE ABSORPTION COEFFICIENT OF NO_2

by
K. G. MUELLER

THIS RESEARCH HAS BEEN SPONSORED BY THE DEFENSE ATOMIC SUPPORT AGENCY
UNDER NWER 12.015

Lockheed

MISSILES & SPACE COMPANY

A GROUP DIVISION OF LOCKHEED AIRCRAFT CORPORATION

SUNNYVALE, CALIFORNIA

FOREWORD

This report compiles the available data on the absorption coefficient of NO_2 and summarizes the results of experimental and theoretical publications which are essential for further investigations of the absorption coefficient of NO_2. The work described here was supported by DASA under Contract DA 49-146-XZ-198 and carried out in the Physical Sciences Laboratory of Lockheed Missiles & Space Company under the direction of Dr. R. K. M. Landshoff.

ABSTRACT

The basic chemical reactions of NO_2 which are active during emission and absorption experiments are given. In the thermal decomposition, the transient species NO_3 is involved which can obscure the optical measurements of NO_2 for wavelengths $> 5,500$ Å. The present knowledge of the energy levels of NO_2 is described and used as the basis for a theoretical prediction of the absorption coefficient at high temperatures. The different descriptions of the absorption used in the literature are reduced to an absorption coefficient $\bar{\kappa}_\nu$ (cm^2/g). The available experimental data of $\bar{\kappa}_\nu$ are listed in a table and presented visually in a figure. By means of a graphical extrapolation, the ranges of wavelengths between 2,500 – 8,000 Å and of temperatures from between 300 – 3,000°K are covered.

CONTENTS

ILLUSTRATIONS

TABLES

Section 1
INTRODUCTION

Recent investigations of air at high temperatures have stressed the effect of the gas NO_2 on the optical properties of air. To calculate this effect, both the concentration and the absorption coefficient of NO_2 have to be known. The equilibrium concentration of NO_2 in air at different temperatures and densities have been calculated by Gilmore (Ref. 1); however, only a few experimental data of the absorption coefficient of NO_2 at high temperature are available, some of them only in the form of unpublished reports or private communication.

This report undertakes a first step toward filling the need for a comprehensive description of the absorption coefficient by

- Compiling available experimental data, including some of the unpublished material
- Extrapolating these data to higher temperatures
- Presenting those physical and chemical properties of NO_2 which are pertinent to experimental and theoretical research on the absorption of NO_2

Nitrogen dioxide, a gas of red brown color, has a molecular weight of 46.01 g.* According to the formula

$$2NO_2 \rightleftarrows N_2O_4 \qquad (1.1)$$

the dimer N_2O_4 can be formed. With decreasing temperature, the equilibrium is shifted to the right side. Under atmospheric pressure, the equilibrium mixture NO_2/N_2O_4 condenses at 294°K and solidifies at 262°K (Ref. 2). The liquid phase is yellow, the solid phase colorless. Extrapolated to normal conditions (273.16°K and 1 atm), the gas NO_2 has density 2.053×10^{-3} g cm^{-3}.

*Table of atomic weights 1961, based on Carbon 12.

Section 2

BASIC CHEMICAL REACTIONS

In this section we discuss the basic reactions of NO_2 pertinent to the optical investigation.

2.1 DIMERIZATION

Giauque and Kemp (Ref. 3) investigated the dimerization (1.1) on the basis of the experimental values given by Wourtzel (Ref. 4), Bodenstein and Boës (Ref. 5), and Verhock and Daniels (Ref. 6). Giauque and Kemp find the following heat of reaction at 0°K (dissociation energy of N_2O_4)

$$\Delta H_o^o = + 12.875 \text{ kcal/mole}$$

$$= + 0.56 \text{ ev/}N_2O_4 \text{ molecule}$$

In Table 1, the experimental data (Ref. 5), denoted by a prime, of the equilibrium constant

$$K_p = \frac{p_{NO_2}^2}{p_{N_2O_4}} \tag{2.1}$$

of the degree α of dissociation, and the data of K_p, corrected by Giauque and Kemp for the gas imperfection, are given. The dissociation constant α is related to the equilibrium constant K_p by the formula

$$\frac{K_p}{p} = \frac{4\alpha^2}{1 - \alpha^2} \tag{2.2}$$

Table 1

EXPERIMENTAL DATA OF THE EQUILIBRIUM CONSTANT, K_p', OF THE DEGREE OF DISSOCIATION, α', AND CORRECTED VALUES OF THE EQUILIBRIUM CONSTANT, K_p, FOR THE REACTION $2NO_2 \rightleftharpoons N_2O_4$

Temperature (°K)	log K'	α'	log K	Temperature (°K)	log K'	α'	log K
338.69	0.351	0.6390	0.363	281.82	-1.449	0.1593	-1.427
339.53	0.379	0.5811	0.396	282.58	-1.394	0.1934	-1.380
341.02	0.407	0.6338	0.421	284.56	-1.372	0.1473	-1.340
342.57	0.459	0.7326	0.469	285.04	-1.316	0.1823	-1.297
342.82	0.445	0.7734	0.452	285.83	-1.273	0.2179	-1.261
343.41	0.474	0.6473	0.489	286.07	-1.323	0.1443	-1.285
344.19	0.493	0.6910	0.506	287.89	-1.193	0.2354	-1.182
351.50	0.681	0.8025	0.693	288.42	-1.185	0.2072	-1.168
352.56	0.696	0.8443	0.706	288.85	-1.197	0.1591	-1.161
353.21	0.709	0.7412	0.725	289.56	-1.137	0.2483	-1.126
353.91	0.732	0.7714	0.747	291.17	-1.138	0.1757	-1.107
356.03	0.784	0.7559	0.802	291.82	-1.091	0.1953	-1.067
356.60	0.798	0.7333	0.818	293.05	-1.022	0.2761	-1.012
361.96	0.903	0.8899	0.916	294.20	-1.007	0.1773	-0.969
362.41	0.949	0.8708	0.964	295.09	-0.951	0.2599	-0.937
363.26	0.932	0.8005	0.951	297.44	-0.881	0.2174	-0.854
364.36	0.962	0.8183	0.981	302.07	-0.729	0.2763	-0.711
366.84	1.024	0.8524	1.044	302.64	-0.749	0.3096	-0.737
369.12	1 079	0.8196	1.103	306.24	-0.589	0.2655	-0.563
372.12	1.139	0.8780	1.160	305.84	-0.612	0.2887	-0.596
372.98	1.146	0.9293	1.165	305.97	-0.587	0.4045	-0.580
373.29	1.145	0.8566	1.169	313.48	-0.351	0.4873	-0.344
374.62	1.214	0.9189	1.234	313.54	-0.347	0.4392	-0.338
374.68	1.184	0.8727	1.209	317.00	-0.291	0.3477	-0.270
383.19	1.352	0.8992	1.382	315.95	-0.284	0.4081	-0.271
384.94	1.378	0.9092	1.410	316.47	-0.274	0.3883	-0.258
385.34	1.444	0.9016	1.482	320.29	-0.159	0.4192	-0.143
386.96	1.425	0.9270	1.459	323.96	-0.043	0.6019	-0.036
387.49	1.412	0.9575	1.439	324.15	-0.036	0.5519	-0.027
390.84	1.543	0.9571	1.581	326.00	0.014	0.4476	0.032
394.85	1.572	0.9367	1.612	326.24	0.015	0.5136	0.027
395.33	1.562	0.9312	1.600	326.76	0.024	0.4912	0.038
398.22	1.660	0.9536	1.684	334.88	0.255	0.5655	0.270
403.93	1.744	0.9526	1.774	334.87	0.254	0.7105	0.261
				335.51	0.276	0.6681	0.286

This relationship is shown graphically in Fig. 1. Due to the gas imperfection, the equilibrium constant K_p shows a slight dependence on the total pressure, p (Ref. 6).

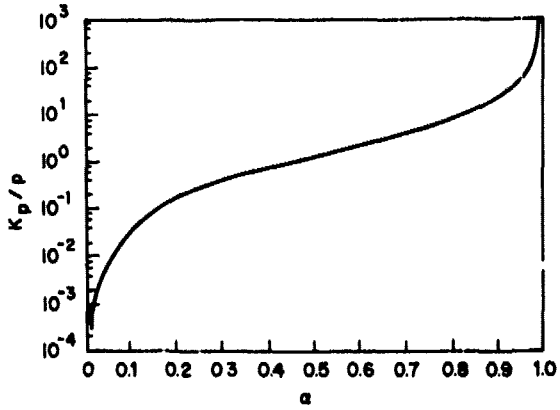

Fig. 1 Degree of Dissociation, α, as a Function of the Quotient, K_p/p

2.2 THERMAL DECOMPOSITION (PYROLYSIS)

Huffman and Davidson (Ref. 7) describe the thermal decomposition of NO_2 in a mixture of argon and NO_2 by two reaction paths. These are

$$NO_2 \overset{M}{\rightleftharpoons} NO + O \tag{2.3}$$

with

$$NO_2 + O \rightleftharpoons NO + O_2 \tag{2.4}$$

where reaction (2.4) is considered fast compared to reaction (2.3), and by

$$2NO_2 \rightleftharpoons 2NO + O_2 \tag{2.5}$$

For the bimolecular path (2.5), the authors assume the mechanism

$$2NO_2 \rightleftharpoons NO_3 + NO \tag{2.6}$$

and

$$NO_2 + NO_3 \rightleftharpoons NO_2 + O_2 + NO \tag{2.7}$$

with the transient species NO_3.

In a more recent publication, Alyea (Ref. 8) proposes two further reactions which involve NO_3 .

The rate of pyrolysis was found by Huffman and Davidson (Ref. 7) as

$$\frac{d[NO_2]}{dt} = -3.06 \times 10^{13} \exp(-65,400/RT)\,[NO_2]\,[M] - 2.5 \times 10^{10} \exp(-25,000/RT)\,[NO_2]^2 \qquad (2.8)$$

where the concentrations $[NO_2]$ and $[M]$ are measured in mole/liter. The dependence of $[NO_3]$ on the time is not yet known.

2.3 CHEMILUMINESCENT REACTIONS

The formation ($\overleftarrow{2.3}$) of NO_2 leads to an excited state, namely

$$NO + O \overset{M}{\rightleftarrows} NO_2^* \qquad (2.9)$$

The transition to the ground state is connected with radiation, extending from 3,975 to 6,000 Å, a process responsible for the green "air afterglow." Stoddard (Ref. 9) and Newman (Ref. 10) investigated the band structure of this chemiluminescent spectrum; a detailed discussion is given by Broida, Schiff, and Sugden (Ref. 11). From the short wavelength cutoff of the spectrum at 3,975 Å, Broida et al. derived a heat of reaction at 0°K (dissociation energy) as follows:

$$\Delta H_o^o = -71.2 \pm 0.1 \text{ kcal/mole } NO_2$$
$$= -3.09 \pm 0.04 \text{ ev/molecule } NO_2$$

Altshuller (Ref. 12), in a thermodynamic investigation of the process,

$$NO_2 \rightleftarrows \frac{1}{2} O_2 + NO \tag{2.10}$$

with

$$\Delta H_o^o = -12.715 \text{ kcal/mole}$$

obtained a similar value using a rigid rotator harmonic oscillator model for NO_2. The results of his calculations are shown in Table 2. From the reaction (2.10) and the reaction

$$\frac{1}{2} O_2 \rightleftarrows O \tag{2.11}$$

with

$$\Delta H_o^o = -58.6 \text{ kcal/mole}$$

the value

$$\Delta H_o^o = -71.3 \text{ kcal/mole}$$
$$= -3.09 \text{ ev/molecule } NO_2$$

for reaction (2.3) can be found.

Another chemiluminescent reaction is given by

$$NO + O_3 \rightleftarrows NO_2 + O_2 \tag{2.12}$$

The emission spectrum of this reaction, tentatively attributed to an excited state of NO_2, extends from 5,900 to 10,850 Å and shows bands superimposed on a continuum (Greaves and Garvin, Ref. 13). The short-wavelength cutoff at 16,935 cm^{-1} corresponds to the heat of reaction (2.12). The thermodynamic properties of this reaction, calculated by Altshuller (Ref. 12), are given in Table 3.

Table 2

THERMODYNAMIC PROPERTIES FOR THE REACTION $NO + \frac{1}{2} O_2 \rightleftarrows NO_2$

Temperature (°K)	$-\frac{H^o - H^o_o}{T}$ cal/deg/mole	$-\frac{F^o - H^o_o}{T}$ cal/deg/mole	ΔH^o kcal/mole	ΔF^o kcal/mole	log K	K
200	2.927	13.754	-13.30	-9.964	10.89	7.76×10^{10}
250	2.804	14.388	-13.42	-9.118	7.971	9.35×10^{7}
298.16	2.663	14.869	-13.51	-8.282	6.070	1.17×10^{6}
300	2.656	14.889	-13.51	-8.248	6.017	1.04×10^{6}
350	2.509	15.286	-13.59	-7.365	4.598	3.96×10^{4}
400	2.346	15.613	-13.65	-6.470	3.534	3.42×10^{3}
500	2.046	16.104	-13.74	-4.663	2.038	1.09×10^{2}
600	1.776	16.454	-13.78	-2.843	1.036	1.09×10^{1}
700	1.543	16.709	-13.80	-1.019	0.318	2.08
800	1.344	16.905	-13.79	0.809	-0.221	0.601
900	1.180	17.056	-13.78	2.635	-0.640	0.229
1000	1.041	17.173	-13.76	4.458	-0.974	0.106
1100	0.922	17.268	-13.73	6.280	-1.248	5.65×10^{-2}
1200	0.823	17.344	-13.70	8.098	-1.474	3.36×10^{-2}
1300	0.736	17.407	-13.67	9.914	-1.667	2.15×10^{-2}
1400	0.663	17.454	-13.64	11.721	-1.830	1.48×10^{-2}
1500	0.601	17.502	-13.62	13.538	-1.972	1.07×10^{-2}

Table 3

THERMODYNAMIC PROPERTIES FOR THE REACTION $NO + O_3 \rightleftarrows NO_2 + O_2$

Temperature (°K)	$-\frac{H^o - H^o_o}{T}$ cal/deg/mole	$-\frac{F^o - H^o_o}{T}$ cal/deg/mole	ΔH^o kcal/mole	ΔF^o kcal/mole	log K	K
200	0.536	0.362	-47.46	-47.27	51.65	4.47×10^{51}
250	0.521	0.469	-47.48	-47.22	41.29	1.95×10^{41}
298.16	0.525	0.570	-47.51	-47.17	34.57	3.72×10^{34}
300	0.524	0.575	-47.51	-47.17	34.36	2.29×10^{34}
350	0.551	0.659	-47.54	-47.11	29.42	2.63×10^{29}
400	0.567	0.730	-47.58	-47.05	25.70	5.01×10^{25}
500	0.604	0.862	-47.65	-46.91	20.50	3.16×10^{20}
600	0.615	0.977	-47.72	-46.76	17.03	1.07×10^{17}
700	0.611	1.067	-47.78	-46.60	14.55	3.55×10^{14}
800	0.593	1.152	-47.83	-46.42	12.68	4.79×10^{12}
900	0.571	1.222	-47.87	-46.24	11.23	1.70×10^{11}
1000	0.546	1.282	-47.90	-46.06	10.07	1.17×10^{10}
1100	0.522	1.335	-47.93	-45.88	9.115	1.30×10^{9}
1200	0.498	1.380	-47.95	-45.69	8.320	2.09×10^{8}
1300	0.473	1.418	-47.97	-45.50	7.648	4.45×10^{7}
1400	0.451	1.452	-47.98	-45.31	7.074	1.19×10^{7}
1500	0.430	1.483	-48.09	-45.12	6.573	3.74×10^{6}

Section 3
FORMATION OF IONS

3.1 POSITIVE ION NO_2^+

Nakayama, Kitamura, and Watanabe (Ref. 14) analyzed the ultraviolet-absorption spectrum, finding a Rydberg series of band systems which leads to an ionization potential

$$U_a = 11.62 \text{ ev} \qquad \text{(Rydberg series)}$$

From the ionization coefficient of the ultraviolet-radiation, the authors derive the potentials

$$U_b = 10.83 \pm 0.02 \text{ ev} \qquad \text{(photo ionization)}$$

$$U_c = 9.75 \pm 0.05 \text{ ev} \qquad \text{(photo ionization)}$$

The value U_b is explained by the reaction

$$NO_2 \rightleftharpoons NO^+ + O^- \qquad (3.1)$$

whereas U_c is interpreted as the ionization potential for a nonvertical 0−0 transition. A thermodynamic estimate with 3.09 ev for the dissociation energy of NO_2, 9.25 ev for the ionization energy of NO (Ref. 15), and 1.46 ev for the electron affinity of O^- (Ref. 16) yields 10.88 ev for the reaction (3.1).

From electron-impact measurements, Kiser and Hisatsune (Ref. 17) derive

$$U_d = 11.27 \pm 0.17 \text{ ev} \qquad \text{(electron impact)}$$

The ionization by electron impact is regarded as a vertical transition corresponding to the Franck-Condon principle. The values U_a and U_d should agree.

3.2 NEGATIVE ION NO_2^-

Fox (Ref. 18) measured the formation of negative ions in NO_2 by electron attachment; the only ion of appreciable quantity was O^-. The author estimated the cross section for attachment to 10^{-18} cm^2 for O^- and 10^{-20} cm^2 for NO_2^-.

Branscomb (Ref. 19) found no detectable photo detachment of NO_2^- ions at the wavelength of 5,200 Å, which indicates for the vertical detachment either a very small cross section or an energy larger than 2.5 ev.

Section 4

QUANTUM MECHANICAL DESCRIPTION

4.1 STRUCTURE

The structure of NO_2 was measured by electron diffraction (Claesson et al., Ref. 20) by infrared spectroscopy (Moore, Ref. 21), and by microwave spectroscopy (Bird, Ref. 22). According to these measurements, NO_2 is a bent molecule with the valance angle

$$\measuredangle \text{ONO} = 134°$$

and the bond length

$$r_{N-O} = 1.19 \text{ Å}$$

Discrepancies of < 1 percent between the results of the different methods stem partly from the fact that in the experiments not the equilibrium structure but an average structure becomes effective (Laurie and Herschbach, Ref. 23).

4.2 SYMMETRY PROPERTIES

A nonlinear or bent molecule of the type XY_2 possesses two symmetry planes $\sigma_v(xz)$ and $\sigma_v(yz)$, i.e., the xz-plane and the yz-plane, and a twofold symmetry axis $C_2(z)$, i.e., the z-axis (Fig. 2). The symmetry axis is introduced as the z-axis. In the literature, the use of the x- and the y-axis varies. We follow the notation of Mulliken (Ref. 24) with the XY_2 molecule lying in the yz-plane. Herzberg (Ref. 25) uses a different notation with the XY_2 molecule lying in the xz-plane.

Because of these symmetry elements, the molecule is classified as belonging to the point group C_{2v}. Each of these symmetry elements induces a symmetry operation.

The twofold symmetry axis gives rise to a rotation about the z-axis by an angle of 180°. The $\sigma_v(xz)$-plane corresponds to a reflection at the xz-plane, which is a coordinate transformation in which y is replaced by -y. Analog $\sigma_v(yz)$ is connected with the reflection at the yz-plane.

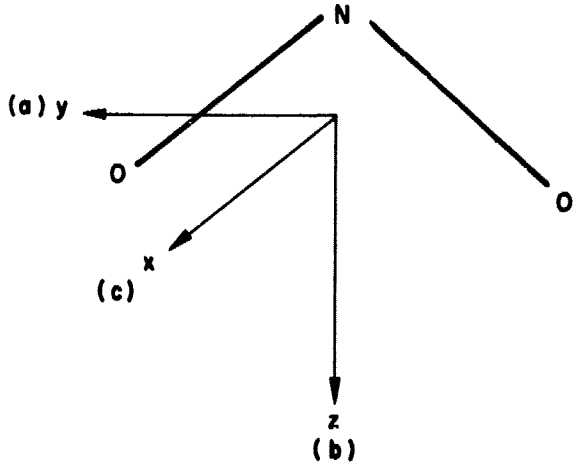

Fig. 2 Center of Mass Coordinate System x, y, z and Principal Axes a, b, c, of the Inertia Ellipsoid

With the identity operation, I, there exist the operations

$$I\ ,\ C_2(z)\ ,\ \sigma_v(xz)\ ,\ \sigma_v(yz)$$

During each operation, the electronic and vibrational eigenfunctions can only be changed by a factor ± 1. This leads to the classification A_1, A_2, B_1, B_2 of the electronic and vibrational eigenfunctions (Table 4).

For the classification of the rotational levels, we have to consider that NO_2 belongs to the asymmetric top molecules. All three principal moments of inertia are different, i.e.,

$$I_A < I_B < I_C$$

Table 4

SYMMETRY TYPES FOR THE POINT GROUP C_{2v}

	I	$C_2(z)$	$\sigma_v(xz)$	$\sigma_v(yz)$
A_1	+1	+1	+1	+1
A_2	+1	+1	-1	-1
B_1	+1	-1	+1	-1
B_2	+1	-1	-1	+1

The inertia ellipsoid possesses three mutually perpendicular twofold symmetry axes, C_2^a, C_2^b, and C_2^c, where each of the axes a, b, c is directed along one of the axes x, y, z of the body system. The detailed correlation depends on the relative magnitude of I_x, I_y, and I_z. Because of this symmetry character, the inertia ellipsoid belongs to the point group V (or D_2). We now regard the operations

$$I\ ,\ C_2^a\ ,\ C_2^b\ ,\ C_2^c$$

and ask if the rotational eigenfunctions remain unchanged or change their sign during such an operation. The possible cases are given in Table 5, with the classifications of Mulliken (Ref. 24) and of Dennison (Ref. 26) who regards only the operations C_2^c and C_2^a.

Besides these classifications, we distinguish symmetric (s) and antisymmetric (a) states with respect to an exchange of the two oxygen molecules.

Table 5

SYMMETRY TYPES FOR THE POINT Group $D_2 \equiv V$

Dennison	Mulliken	C_2^c	C_2^b	C_2^a
++	A	+	+	+
+-	B_c	+	-	-
-+	B_a	-	-	+
--	B_b	-	+	-

4.3 ROTATIONAL ENERGY LEVELS

For an asymmetric top molecule, the total angular momentum $\vec{J}$ in a given energy level is fixed in space. Its magnitude $\sqrt{J(J+1)}\hbar$ may be described by the quantum number J. To each value of J there exists $2J + 1$ sublevels, which are distinguished by subscript

$$\tau = -J \ldots +J$$

These quantum numbers τ have no longer physical meaning as in the case of the symmetric top, where they can be interpreted as the projection of $\vec{J}$ on the symmetry axis of the top. One can only say that $\tau = -J$ corresponds approximately to a rotation about the axis of least moment of inertia and that $\tau = +J$ corresponds approximately to a rotation about the axes of largest moment of inertia.

In Fig. 3, the energy levels of the asymmetric top with

$$I_A < I_B < I_C$$

are compared with those of prolate symmetric top

$$I_A < I_B = I_C$$

and those of an oblate symmetric top

$$I_A = I_B < I_C$$

As a good approximation, the rotational levels of NO_2 may be described by the prolate symmetric top model with the quantum number J and K, where K is the magnitude of the projection of J on the symmetry axis.

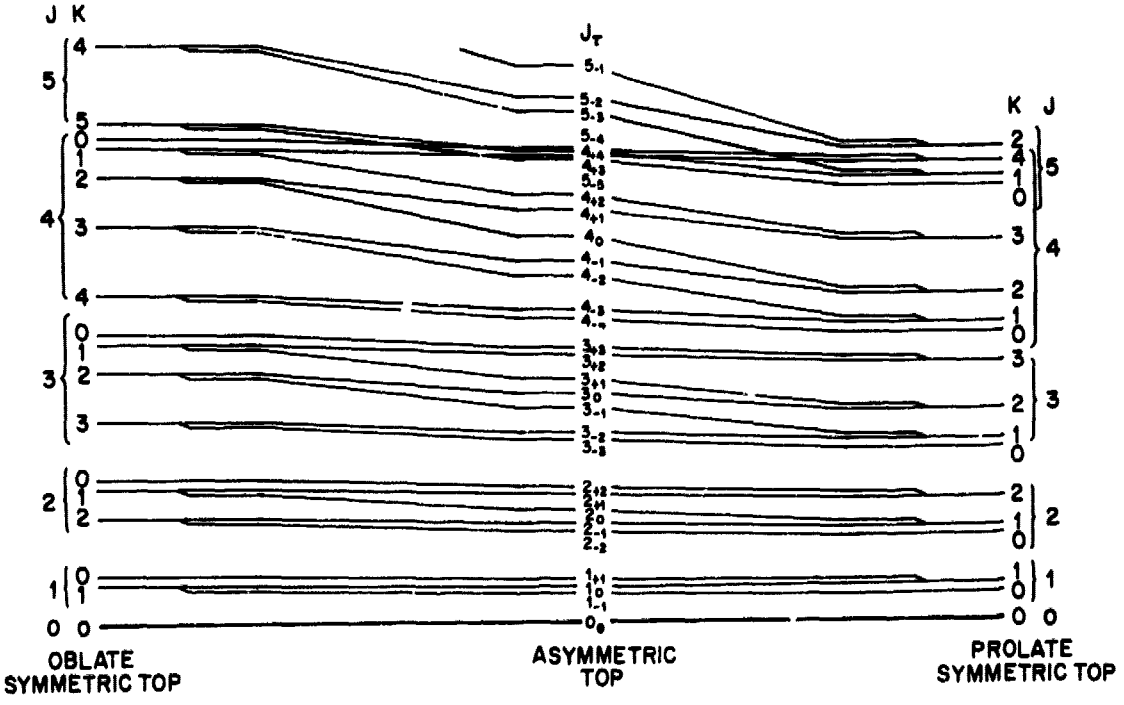

Fig. 3 Energy Levels of the Asymmetric Top Molecule – Correlation to Those of Symmetric Top Molecules

For more detailed discussion we refer to Herzberg (Ref. 25).

4.4 VIBRATIONAL ENERGY LEVELS

The bent molecule NO_2 possesses three normal modes of vibration (Fig. 4). During these vibrations, the center of mass rests. For the dissociation, only ν_1 and ν_3 are of interest; ν_2 mainly represents a bending vibration. We see that the normal vibration ν_1 and ν_2 are of the symmetric type A_1, whereas ν_3 belongs to the type B_2. According to the notation of Herzberg, ν_3 belongs to the type B_1.

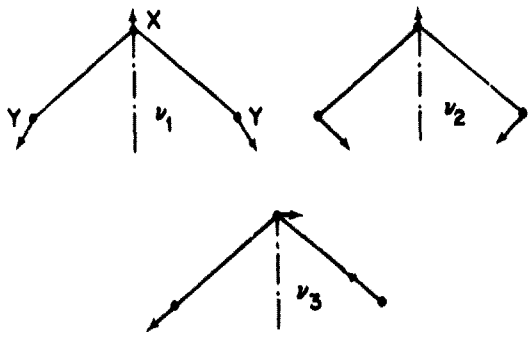

Fig. 4 Normal Modes of Vibration for a Plane Molecule XY_2

Moore (Ref. 21), in his analysis of the infrared spectrum, found the energy of the vibrational levels to be

$$G(v_1, v_2, v_3) = \sum_{i=1}^{3} \omega_i \left(v_i + \frac{1}{2}\right) + \sum_{i=1}^{j} \sum_{j=1}^{3} x_{ij} \left(v_i + \frac{1}{2}\right)\left(v_j + \frac{1}{2}\right) \qquad (4.1)$$

where

$$\omega_1 = 1361.4 \pm 1.7 \text{ cm}^{-1} \; ; \; x_{11} = -7.1 \pm 0.3 \text{ cm}^{-1} \; ; \; x_{22} = -8.1 \pm 3.3 \text{ cm}^{-1}$$

$$\omega_2 = 770.2 \pm 6.6 \text{ cm}^{-1} \; ; \; x_{12} = -16.0 \pm 3.3 \text{ cm}^{-1} \; ; \; x_{23} = -8.2 \pm 3.3 \text{ cm}^{-1}$$

$$\omega_3 = 1668.6 \pm 1.7 \text{ cm}^{-1} \; ; \; x_{13} = -33.4 \pm 0.1 \text{ cm}^{-1} \; ; \; x_{33} = -15.9 \pm 0.2 \text{ cm}^{-1}$$

The potential energy of the vibrating molecule NO_2 in the vicinity of the equilibrium configuration can be expressed by

$$V = \frac{1}{2}\left(\lambda_1 \xi_1^2 + \lambda_2 \xi_2^2 + \lambda_3 \xi_3^2\right) \qquad (4.2)$$

where λ_i are constants and ξ_i the normal coordinates.

We now compare Eq. (4.2) with the potential energy of a diatomic molecule, for which V is only a function of one variable ξ. For the diatomic molecule, a simple graphical representation of the potential curve $V(\xi)$ can be given. This is no longer possible for a three-atomic molecule, where a potential curve can be constructed for each normal coordinate ξ_i. For some qualitative discussion, however, using one single potential curve averaged over the different normal coordinates can be instructive.

4.5 ELECTRONIC ENERGY LEVELS

Mulliken (Ref. 27), Walsh (Ref. 28), Mulliken (Ref. 29), McEwen (Ref. 30), and Green and Linnett (Ref. 31) made a molecular orbital calculation of NO_2 which gives a rough picture of the electronic energy levels. These molecular orbitals

$$\Psi = \sum c_i \psi_i \tag{4.3}$$

are constructed by linear combinations of atomic orbitals ψ_i (LCAO) of the three atoms of NO_2. The contributing atomic orbitals ψ_i of the 23 electrons of NO_2 are

$$\begin{aligned} &\text{N: } 1s^2 , 2s^2 , 2p^3 \\ &\text{O: } 1s^2 , 2s^2 , 2p^4 \\ &\text{O': } 1s^2 , 2s^2 , 2p^4 \end{aligned}$$

The six 1s electrons are regarded as localized at the atoms and thus can be ignored. Thus the following orbitals can contribute

$$\begin{aligned} &\text{N: } 2s , 2p_x , 2p_y , 2p_z \\ &\text{O: } 2s , 2p_x , 2p_{\parallel} , 2p_{\perp} \\ &\text{O': } 2s , 2p_x , 2p_{\parallel} , 2p_{\perp} \end{aligned}$$

where $p_{\parallel}$ and $p_{\perp}$ are parallel and perpendicular to the N-O bond, and the two O-atoms are distinguished by O and O'. The positive direction of y, z, ∥, and ⊥ for the different atoms are demonstrated in Fig. 5.

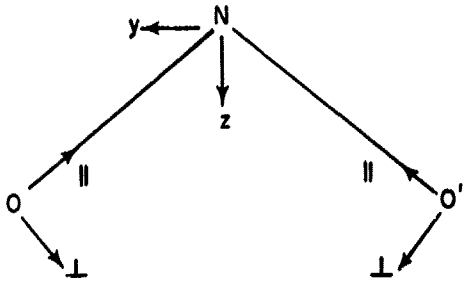

Fig. 5 Coordinate System Used for the MO Calculations

Only those combinations of atomic orbitals need be taken into account which belong to one of the symmetry species a_1, a_2, b_1, or b_2. For the designation of the symmetry of one-electron molecular orbitals, small letters are used.

Figure 6, taken from Mulliken (Ref. 27), presents a general picture of the energy levels of an average molecule AO_2 in which the influence of the number of electrons and of the apex angle is demonstrated.

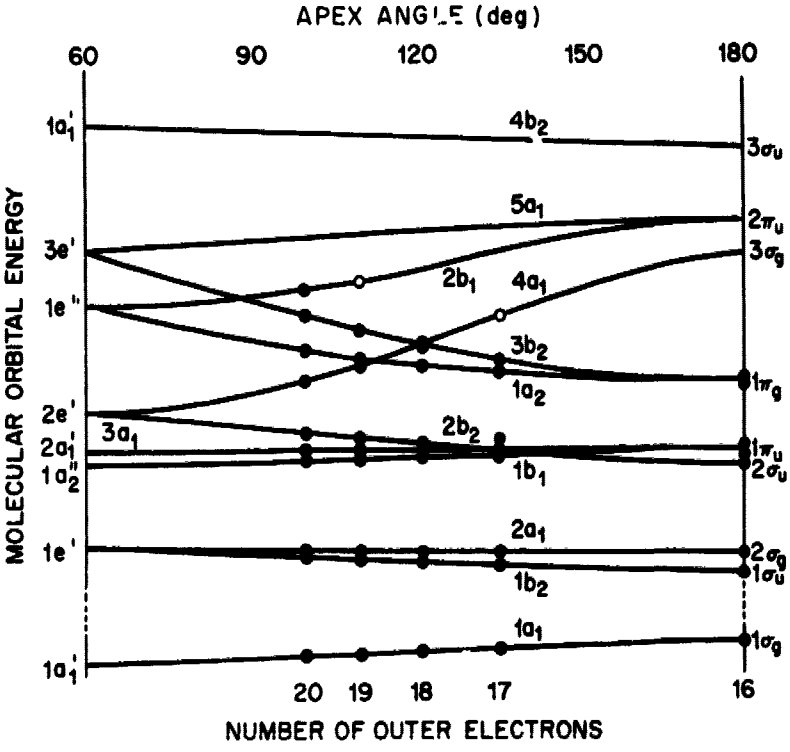

Fig. 6 Calculated Energy Levels of an Average Molecule AO_2 as a Function of the Number of Electrons (in Molecular Orbitals) and of the Apex Angle

A more recent calculation was done by McEwen (Ref. 30) and by Green and Linnett (Ref. 31); the orbitals are given in Table 6. Since in Ref. 31 the positive direction of the coordinate axes

Table 6

ORBITAL COEFFICIENTS CALCULATED BY GREEN AND LINNETT (UPPER VALUES) AND BY MC EWEN (LOWER VALUES)

	N				$(O \pm O')/\sqrt{2}$			
	2s	$2p_x$	$2p_y$	$2p_z$	2s	$2p_x$	$2p_{\|\|}$	$2p_\perp$
$5a_1$	(+) 0.347			(−) 0.603			(−) 0.344	(−) 0.626
$4a_1$	(−) 0.410 + 0.314			(+) 0.471 − 0.511	+0.01		(−) 0.565 − 0.410	(+) 0.539 + 0.680
$3a_1$	(−) 0.198 + 0.257			(+) 0.626 − 0.639			(+) 0.749 − 0.180	(+) 0.089 − 0.710
$2a_1$	(+) 0.820			(+) 0.129			(+) 0.042	(+) 0.556
$4b_2$			(+) 0.752				(−) 0.157	(−) 0.640
$3b_2$			(±) 0.0				(−) 0.971 − 0.140	(+) 0.238 + 0.990
$2b_2$			(+) 0.660				(+) 0.180	(+) 0.730
$2b_1$		(+) 0.777 + 0.798				(−) 0.628 − 0.603		
$1b_1$		(+) 0.628 + 0.603				(+) 0.777 − 0.798		
$1a_2$						(+) 1.000 + 1.000		

are not given, the sign of these orbital coefficients are given in parenthesis. The unpaired electron is placed in the $4a_1$ level, so that in this approximation the ground state is given by

$$1a_1^2, 1b_2^2, 2a_1^2, 2b_2^2, 1b_1^2, 3a_1^2, 1a_2^2, 3b_2^2, 4a_1$$

where the 1s electrons are neglected. Figure 7 shows the energy of the levels relative to the ground level $4a_1$ of the unpaired electron. Because of the inherent assumptions

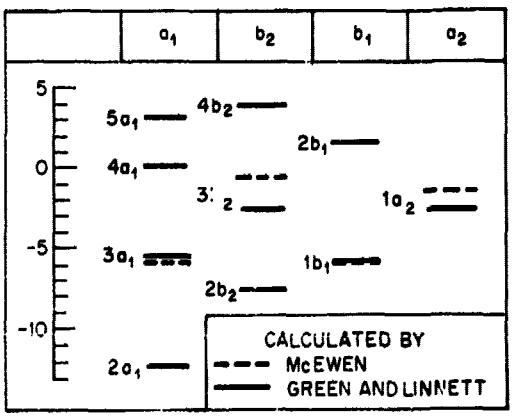

Fig. 7 Energy Levels Calculated With Respect to the Ground State $4a_1$

of those calculations, the results are of a semiquantitative character and cannot be used to predict the electronic spectrum.

4.6 VIBRATIONAL STRUCTURE OF ELECTRONIC TRANSITIONS

During an electronic transition of NO_2, the three normal coordinates ξ_i'' transform into ξ_i' (Soshnikov, Ref. 32), i.e.,

$$\xi_1' = a_{11}\xi_1'' + a_{12}\xi_2'' + C_1 \tag{4.4}$$

$$\xi_2' = a_{21}\xi_1'' + a_{22}\xi_2'' + C_2 \tag{4.5}$$

$$\xi_3' = \xi_3'' \tag{4.6}$$

This means that with an electronic transition, a displacement (C_1 and C_2) and a rotation of the two symmetric coordinates ξ_1 and ξ_2 can be connected. The third (antisymmetric) coordinate transforms into itself. In addition, the normal frequencies ν_i may change. Because of Eq. (4.6), the antisymmetric coordinate ξ_3 may be disregarded.

From the spectroscopic data of NO_2, Broida, Schiff, and Sugden (Ref. 11) derived the qualitative potential curves of Fig. 8. The authors account for four different electronic states. A simpler diagram with two curves – one for the ground state and one for the excited state – was proposed by Soshnikov (Ref. 33).

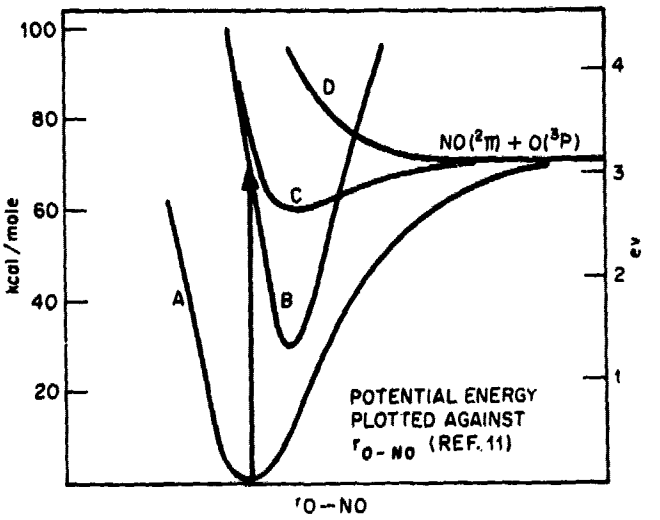

Fig. 8 Potential Energy Curves for the Dissociation $NO_2 \rightarrow NO + O$

Section 5

DERIVATION OF THE ABSORPTION COEFFICIENT

5.1 BASIC EQUATIONS OF RADIATIVE TRANSFER

Emission and absorption of radiation are governed by the equation of radiative transfer

$$\frac{dI_\nu}{ds} = \rho j_\nu - \rho \kappa_\nu I_\nu \tag{5.1}$$

where

I_ν = flux of radiation
per unit frequency interval about ν
per unit solid angle in the direction of $\vec{\Omega}$
per unit area normal to the direction $\vec{\Omega}$
in ergs/cm^2

j_ν = emission of radiation
per unit frequency interval about ν
per unit solid angle in the direction $\vec{\Omega}$
per unit mass of the radiating gas (NO_2)
in ergs/g

κ_ν = absorption coefficient of the gas (NO_2)
for radiation of the frequency, ν
in cm^2/g

ρ = (mass) density of the radiating gas (NO_2)
in g/cm^3

ds = differential of the path length in the direction of $\vec{\Omega}$

For local thermodynamic equilibrium, the emission j_ν is given by

$$j_\nu = \kappa_\nu (1 - e^{-h\nu/kT}) B_\nu + e^{-h\nu/kT} \kappa_\nu I_{,\nu} \tag{5.2}$$

with the Planck function

$$B_\nu = \frac{2h\nu^3}{c^2} \frac{e^{-h\nu/kT}}{1 - e^{-h\nu/kT}} \tag{5.3}$$

The first term in Eq. (5.2) corresponds to the spontaneous and the second term to the induced emission. The induced emission, which is proportional to the flux I_ν, reduces the true absorption κ_ν to the apparent (measurable) absorption κ'_ν

$$\kappa'_\nu = \kappa_\nu(1 - e^{-h\nu/kT}) \tag{5.4}$$

In the investigated temperature and frequency range, the difference between κ_ν and κ'_ν vanishes.

If we can neglect the emission relative to the absorption, as in the case of the absorption experiments, we can integrate Eq. (5.1) and for the decrease of the flux I_ν over the path ℓ we find

$$I_\nu = I_\nu(0)\, e^{-\rho\kappa_\nu \ell} \tag{5.5a}$$

where $I_\nu(0)$ is the original flux. In the literature, there exist several descriptions of the absorption equivalent to Eq. (5.5a), i.e.,

$$I_\nu = I_\nu(0)\, e^{-\sigma n \ell} \tag{5.5b}$$

where σ is the absorption cross section $\left(cm^2/\text{molecule } NO_2\right)$ and n the number density $\left(\text{molecules } NO_2/cm^3\right)$

$$I_\nu = I_\nu(0) \times 10^{-\epsilon c \ell} \tag{5.5c}$$

where ϵ is the extinction coefficient (liter/mole NO_2/cm) and c the concentration (moles NO_2/liter)

$$I_\nu = I_\nu(0) \times 10^{-\alpha p_o \ell} \tag{5.5d}$$

$$I_\nu = I_\nu(0) \times 10^{-k_\alpha p \ell} \tag{5.5e}$$

where α and k_α are the absorption coefficients ($1/cm/mm\ Hg\ NO_2$), p is the pressure ($mm\ Hg\ NO_2$), and p_o the reduced pressure ($mm\ Hg\ NO_2$) on 0°C

$$p_o = \frac{p \times T}{273.16} \tag{5.6}$$

Comparing Eqs. (5.5a) through (5.5e), we find

$$\kappa_\nu = \frac{n}{\rho}\sigma = \frac{N}{M}\sigma = 1.309 \times 10^{22}\,\sigma\left(cm^2/g\ NO_2\right) \tag{5.7}$$

where N is Avogadro's number and M is the molecular weight, and

$$\kappa_\nu = 2.303\,\frac{c}{\rho}\,\epsilon = 50.05\,\epsilon\ \left(cm^2/g\ NO_2\right) \tag{5.8}$$

$$\kappa_\nu = 2.303\,\frac{p}{\rho}\,k_\alpha = 3.121 \times 10^3\,T\,k_\alpha\left(cm^2/g\ NO_2\right) \tag{5.9}$$

$$\kappa_\nu = 2.303\,\frac{p_o}{\rho_o}\,\alpha = 0.8525 \times 10^6\,\alpha\ \left(cm^2/g\ NO_2\right) \tag{5.10}$$

For the emission experiments the relations

$$I_\nu \leq B_\nu \tag{5.11}$$

$$e^{-h\nu/kT} \ll 1 \tag{5.12}$$

hold. Thus we can derive κ_ν from the measured emission by the equation

$$\kappa_\nu = j_\nu\,\frac{c^2}{2h\nu^3}\,e^{h\nu/kT} \quad \text{[See Eqs. (5.2) and (5.3)]} \tag{5.13}$$

In one publication we find the emission j^*_λ in photons/sec/mole/wavelength unit. The following relation exists between j_ν and j^*_λ:

$$j_\nu = j^*_\lambda \frac{h\nu}{M} \frac{\lambda}{\nu} \tag{5.14}$$

5.2 THEORETICAL DERIVATION

We wish to calculate an absorption coefficient which is averaged over the vibrational and rotational structure

$$\bar{\kappa}_\nu = \frac{1}{\Delta\nu} \int_{\nu-(\Delta\nu/2)}^{\nu+(\Delta\nu/2)} \kappa_\nu \, d\nu \tag{5.15}$$

The quantity $\Delta\nu$ is chosen, such that $\bar{\kappa}_\nu$ becomes a smooth curve. For the range of the visible frequencies we assume that only one excited electronic state is involved. If we average over the rotational contribution of the spectrum, we only have to consider transitions from a vibrational level v'' of the electronic ground state to a level v' of the first excited electronic level. The absorption coefficient is given by

$$\rho\bar{\kappa}_\nu = \frac{1}{\Delta\nu} \sum N_{v''} B_{v''\to v'} h\nu_{v''\to v'} \tag{5.16}$$

where $N_{v''}$ is the number density of the state v''. $\nu_{v''\to v'}$ the wave number, and $B_{v''\to v'}$, the Einstein coefficient for induced absorption. For a given value of ν, the sum goes over all transitions $v'' \to v'$, which contribute to $\bar{\kappa}_\nu$ in the interval $\Delta\nu$. By means of the Born-Oppenheimer approximation for the total eigenfunction

$$\Psi = \Psi_c \cdot \Psi_v \cdot \Psi_r \tag{5.17}$$

the Einstein coefficient may be factored into

$$B_{v'' \rightarrow v'} = \frac{8\pi^3}{3h^2c} R_e^2 q(v', v'') \tag{5.18}$$

where $q(v', v'')$ is the Franck-Condon factor

$$q(v', v'') = \left| \int \Psi_v''^* \Psi_v' \, d\tau_v \right|^2 \tag{5.19}$$

$\vec{R}_e$ the electronic transition moment

$$\vec{R}_e = \int \Psi_e''^* \vec{R} \Psi_e' \, d\tau \tag{5.20}$$

and $\vec{R}$ the electric dipole operator.

Since the molecule NO_2 has three normal modes of vibration, the transition

$$v'' \rightarrow v'$$

is written in detail

$$v_1'', v_2'', v_3'' \rightarrow v_1', v_2', v_3'$$

For the three-dimensional harmonic oscillator model with Eqs. (4.4)–(4.6) and

$$\left.\begin{aligned} a_{11} &= a_{22} = 1 \\ a_{12} &= a_{21} = 0 \end{aligned}\right\} \tag{5.21a}$$

$$\left.\begin{aligned} \nu_1' &= \nu_2'' \\ \nu_2' &= \nu_2'' \\ \nu_3' &= \nu_3'' \end{aligned}\right\} \tag{5.21b}$$

Soshnikov (Ref. 32) calculated the Franck-Condon factors $q(v', v'')$ finding the following relations:

$$q_3(v_1', v_1''; v_2', v_2''; v_3', v_3'') = q_2(v_1', v_1''; v_2', v_2'')\,\delta_{v_3' v_3''} \tag{5.22}$$

$$q_2(v_1', v_1''; v_2', v_2'') = q_1(v_1', v_1'') \cdot q_1(v_2', v_2'') \tag{5.23}$$

$$q_1(a,b) = \frac{b!}{a!}\, X^{a-b} e^{-X}\left[\frac{a\ldots(a-b+1)}{b!\;0!} + \ldots + (-1)^{k-1}\,\frac{a\ldots(a-b+k)}{(b-k+1)(k-1)!}\,X^{k-1} + \ldots + (-1)^m\,\frac{X^b}{0!\;b!}\right]^2 \tag{5.24}$$

where δ is the Kronecker symbol and

$$X_1 = \frac{C_i^2 2\pi^2 \nu_i}{h} \tag{5.25}$$

is a measure for the horizontal displacement of the potential curves. Equation (5.24) holds for the first and second normal vibration. Because of Eqs. (4.6) and (5.22), the third normal vibration ν_3 can be neglected.

With the help of Eqs. (5.16) through (5.23), the absorption coefficient $\bar{\kappa}_\nu$ can now be expressed by

$$\rho\bar{\kappa}_\nu = \frac{8\pi^3}{3hc^2} R_e^2 \frac{\nu}{\Delta\nu}\, n\, \frac{1}{Z_1 \cdot Z_2} \sum_{(\Delta\nu)} \exp\left[-\frac{hc}{kT}\,(v_1''\nu_1 + v_2''\nu_2)\right] q_1(v_1', v_1'')\, q_1(v_2', v_2'') \tag{5.26}$$

with the vibrational partition functions

$$Z_i = \frac{1}{1 - e^{-hc\nu_i/kT}} \tag{5.27}$$

and the wave numbers

$$\nu = \nu_e + (v_1' - v_1'')\,\nu_1 + (v_2' - v_2'')\,\nu_2 \tag{5.28}$$

within the interval $\Delta\nu$.

Taking the logarithm of Eq. (5.26), we find

$$\log \frac{\bar{\kappa}_\nu}{\nu} = A + \log \left\{ \frac{1}{Z_1 \cdot Z_2} \sum \exp \left[- \frac{hc}{kT} \left(v_1'' \nu_1 + v_2'' \nu_2 \right) \right] q_1(v_1', v_1'') \, q_1(v_2', v_2'') \right\} \tag{5.29}$$

where the value of A is constant for the described electronic transition of NO_2. For a given set of the displacement parameters C_1 and C_2, we can calculate the logarithm of the right side as a function of ν with T as a parameter, assuming an arbitrary value of ν_e. To adjust these calculated curves for the correct value of ν_e, the curves have to be shifted horizontally. If the exact values for C_1 and C_2 are chosen, the calculated curves become identical to the curves $\log \bar{\kappa}_\nu / \nu$ after horizontal shifting for adjusting of ν_e and after vertical shifting for adjusting of the constant A.

The described application of Eq. (5.29) was used by Soshnikov (Ref. 32) on the extrapolation of $\bar{\kappa}_\nu(T)$ curves from $\bar{\kappa}_\nu$ for room temperature.

5.3 EXPERIMENTAL DATA OF THE ABSORPTION COEFFICIENT

The principal sources of production of an absorption or emission spectrum are

- Shock tubes
- Chemiluminescent reaction (flame, air afterglow)
- Fluorescence

The spectral distribution and the decay of the radiation may be measured.

The absorption coefficient at room temperature has been widely investigated [Dickinson and Baxter (Ref. 34), Holmes and Daniels (Ref. 35), Dixon (Ref. 36), Price and Simpson (Ref. 37), Hall and Blacet (Ref. 38), Mori (Ref. 39), Nakayama, Kitamura, and Watanabe (Ref. 14)]. At higher temperatures, however, only a few data are available [Harris, King, Benedict, and Pearse (Ref. 40), Petty (Ref. 41), Heath and Dieke (Ref. 42), Raizer (Ref. 43), Schott and Davidson (Ref. 44), Huffman and Davidson (Ref. 7), and Alyea (Ref. 8)]. In Table 7, the data derived from these sources are presented.

Table 7

DATA OF THE AVERAGE ABSORPTION COEFFICIENT $\bar{\kappa}_\nu$ (cm^2/g) TAKEN FROM TABLES AND FIGURES OF VARIOUS AUTHORS

Wavelength, λ (Å)	Absorption Coefficient, $\bar{\kappa}_\nu$ (cm^2/g)				
(a)	2000°	2600°	3000°	4000°	5000°
6500	1.1^{3}*	2.4^{3}	2.8^{3}	3.9^{3}	4.7^{3}
(b)	300°	425°	605°	820°	1020°
3500	7.0^{3}	–	–	4.8^{3}	–
4000	8.4^{3}	–	–	6.3^{3}	7.4^{3}
4500	6.5^{3}	5.6^{3}	5.6^{3}	5.0^{3}	6.0^{3}
5000	2.8^{3}	3.4^{3}	3.4^{3}	3.4^{3}	4.2^{3}
5500	1.3^{3}	1.5^{3}	1.9^{3}	1.9^{3}	3.0^{3}
6000	5.6^{2}	7.0^{2}	8.5^{2}	9.0^{2}	1.9^{3}
(c)	300°	800°	1000°	1500°	2000°
4050	8.2^{3}	7.0^{3}	6.5^{3}	5.7^{3}	4.8^{3}
4360	7.2^{3}	5.9^{3}	5.6^{3}	5.0^{3}	4.4^{3}
5460	1.4^{3}	–	2.8^{3}	3.2^{3}	–
(d)	300°	500°	1000°	1500°**	
3660	7.5^{3}	6.8^{3}	6.6^{3}	5.0^{3}	
5460	1.9^{3}	2.1^{3}	2.5^{3}	3.0^{3}	
6500	2.0^{2}	4.0^{2}	8.5^{2}	1.3^{3}	
(e)	297°	400°	500°		
5500	1.3^{3}	1.5^{3}	1.8^{3}		
6000	5.6^{2}	6.5^{2}	8.4^{2}		
6500	1.7^{2}	2.4^{2}	2.8^{2}		
7000	3.7^{1}	5.6^{1}	9.3^{1}		
7500	1.9^{1}	3.7^{1}	5.6^{1}		
8000	7.4^{0}	1.4^{1}	2.3^{1}		
8500	2.8^{0}	3.7^{0}	1.1^{1}		

Wavelength, λ (Å)	Absorption Coefficient, $\bar{\kappa}_\nu$ (cm^2/g)	
(f)	298°	413°
3400	5.1^{3}	–
3500	6.1^{3}	–
3600	7.0^{3}	–
5150 Å 5450	$1.4^{3}-2.3^{3}$	$1.3^{3}-2.6^{3}$
(g)	378°	604°
2666	1.7^{3}	2.6^{3}
2576	1.6^{3}	1.8^{3}
2539	1.3^{3}	1.7^{3}
(h)	298°	
2500	5.0^{2}	
3000	2.0^{3}	
3500	6.5^{3}	
4000	8.4^{3}	
4500	6.5^{3}	
5000	3.7^{3}	
(i)	300°	
4000	8.1^{3}	
4500	6.5^{3}	
5000	3.6^{3}	
5500	1.6^{3}	
6000	6.0^{2}	
6500	2.0^{2}	
7000	7.9^{1}	
(j)	1070° – 1530°	
3600 Å 4200	$-2.47\,T + 9540$	

(a) Raizer
(b) Heath and Dicke
(c) Huffman and Davidson
(d) Schott and Davidson
(e) Heath and Dicke
(f) Petty
(g) Harris, King, Benedict, and Pearse
(h) Hall and Blacet
(i) Dixon
(j) Alyea

*$1.1^{3} = 1.1 \times 10^{3}$
**Extrapolated

The solid curves of Fig. 9a are constructed from these data by means of the relations (5.7) through (5.10). The data of Raizer (Ref. 43), presented by him as likely values without any further reference, are outside the experimentally checked temperature and wavelength region.

From emission curves published recently by Levitt (Ref. 45), and with the help of Eqs. (5.13) and (5.14), we have calculated an absorption coefficient (Fig. 9b) which deviates from the curves of Fig. 9a up to a factor of 5 and which shows in addition a different temperature dependence. Since the emission is rather sensitive to deviation from the equilibrium population, we disregard these data.

In the wavelength region >5,400 Å, the absorption coefficient of NO_3 is 10 to 50 times larger than that of NO_2 (Ref. 44). Because NO_3 is an intermediate product of the thermal decomposition of NO_2, this effect can give rise to experimental errors in the large-wavelength region.

5. EXTRAPOLATION TO HIGH TEMPERATURES

The calculated absorption coefficient [Eq. (5.29)] for the three-dimensional harmonic oscillator may be applied to extrapolate the experimental curves to higher temperatures, adjusting the values of the unknown quantities A, ν_e, X_1, X_2 by comparing the calculated $\bar{\kappa}_\nu/\nu$ to the experimental data.

To account for possible deviations from the model assumption of Eq. (5.21), Soshnikov permitted the quantities A, ν_e, X_1, and X_2 to depend on the wave number ν; he determined this dependence by using the experimental values of $\bar{\kappa}_\nu$ and its first two derivatives as measured at 300°K. The curves of Fig. 9c are derived from his calculations. Practically the same curves have been found for the simple harmonic oscillator model for several values of the normal frequency.

Adjusting the unknown parameters at each frequency is an empirical method to be applied only to small variations of these parameters. For large variations, the

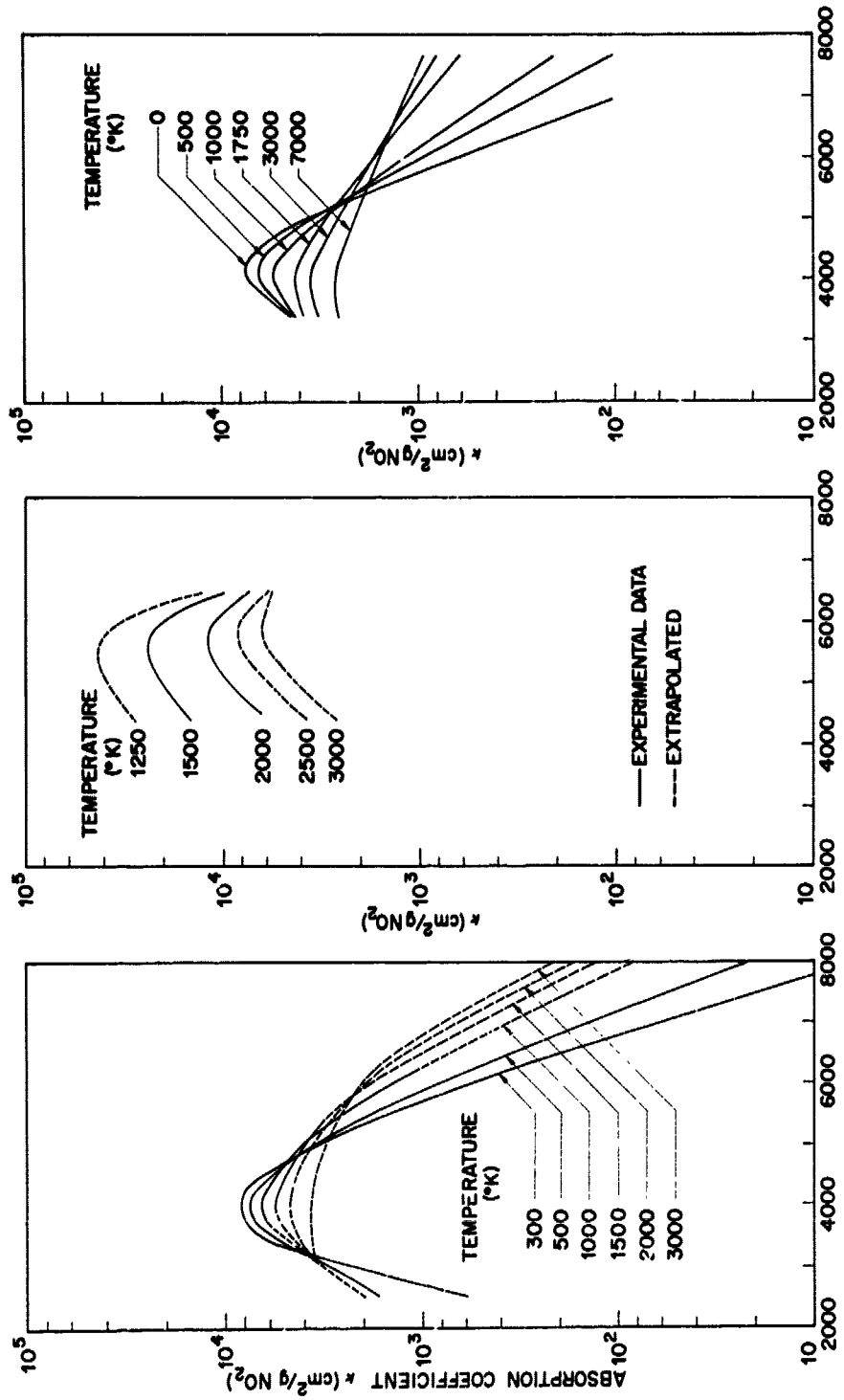

Fig. 9 Absorption Coefficient $\bar{\kappa}_\nu$ of NO_2 as a Function of the Wavelength λ With the Temperature T as a Parameter

simple model of the three-dimensional harmonic oscillator breaks down. Soshnikov (Ref. 32) gives no details about the variation of these parameters.

According to the experimental values, the curves predicted by Soshnikov for wavelengths $\geq 6,000$ Å are too high. With the higher temperature data as a basis for the calculation of the absorption, Eq. (5.29), a better prediction is possible. In this paper we used a simple graphical extrapolation of the experimental data, which is shown in the dotted curves of Fig. 9.

Section 6
CONCLUDING REMARKS

The curves of Fig. 9a represent an average absorption coefficient; the curves actually measured are much more complicated. The value for the average coefficient was obtained graphically: the error of this procedure may be estimated to be ± 10 percent.

For the limited region $3,000 \leq \lambda \leq 6,000$ Å and $300 \leq T \leq 2,000°K$, this averaging process is the main error source. The data beyond this region are uncertain and require checking by further investigations.

The experimental investigation in the region of large wavelength $\lambda \geq 6,000$ Å becomes complicated because of interference with the transient species NO_3.

At $\lambda = 2,500$ Å, the absorption coefficient increases with decreasing λ, up to values of 10^5 cm^2/g. Because of this extreme change of $\bar{\kappa}_\nu$, the averaging process produces large errors and depends strongly on the value of $\Delta\nu$ in Eq. (5.15). For this reason we omitted this region in Fig. 9a.

More reliable extrapolation to higher temperatures ($T > 2,000°K$) can be obtained on the basis of the measured values up to 2,000°K by applying Eq. (5.29).

Section 7
REFERENCES

1. F. R. Gilmore, Equilibrium Composition and Thermodynamic Properties of Air to 24,000°K, Research Memorandum RM-1543, Rand Corporation, Santa Monica, Calif., 1955
2. Landolt–Börnstein, Zahlenwerte und Funktionen aus Physik, Chemie, Astronomie, Geophysik und Technik, Vol. II, 2a, Berlin, Springer, 1960
3. W. F. Giauque and J. D. Kemp, J. Chem. Phys., Vol. 6, p. 40, 1938
4. E. Wourtzel, Compt. rend., Vol. 169, p. 1397, 1919
5. M. Bodenstein and F. Boës, Zeitschrift phys. Chem., Vol. 100, p. 75, 1922
6. F. H. Verhoek and F. Daniels, J. Am. Chem. Soc., Vol. 53, p. 1250, 1931
7. R. E. Huffman and N. Davidson, J. Am. Soc., Vol. 81, p. 2311, 1959
8. F. N. Alyea, The Rate of Pyrolysis of Nitrogen Dioxide in a Shock Tube, Ph.D. Thesis, Stanford University, Stanford, Calif., 1962
9. E. M. Stoddart, Proc. Roy. Soc. A, Vol. 147, p. 454, 1934
10. F. N. Newman, Phil. Mag., Vol. 20, p. 777, 1935
11. H. P. Broida, H. I. Schiff, and T. M. Sugden, Trans. Faraday Soc., Vol. 57, p. 259, 1961
12. A. P. Altshuller, J. Phys. Chem., Vol. 61, p. 251, 1957
13. J. C. Greaves and D. Garvin, J. Chem. Phys., Vol. 30, p. 348, 1959
14. T. Nakayama, M. Y. Kitamura, and K. Watanabe, J. Chem. Phys., Vol. 30, p. 1180, 1959
15. K. Watanabe, J. Chem. Phys , Vol. 22, p. 1564, 1954

16. L. M. Branscomb, D. S. Burch, S. J. Smith, and S. Geltman, Phys. Rev., Vol. 111, p. 504, 1958

17. R. W. Kiser and I. C. Hisatsune, J. Phys. Chem., Vol. 65, p. 1444, 1961

18. R. E. Fox, J. Chem. Phys., Vol. 32, p. 285, 1960

19. L. M. Branscomb, Atomic and Molecular Processes, D. R. Bates, ed., Academic Press, 1962

20. S. Claesson, J. Donohue, and V. Schomaker, J. Chem. Phys., Vol. 16, p. 207, 1948

21. G. E. Moore, J. Opt. Soc. Am., Vol. 43, p. 1045, 1953

22. G. R. Bird, J. Chem. Phys., Vol. 25, p. 1040, 1956

23. V. W. Laurie and D. R. Herschbach, J. Chem. Phys., Vol. 37, p. 1687, 1962

24. R. S. Mulliken, Phys. Rev., Vol. 59, p. 873, 1941

25. G. Herzberg, Molecular Spectra and Molecular Structure II, New York, D. Van Nostrand, 1956

26. D. M. Dennison, Rev. Mod. Phys., Vol. 3, p. 280, 1931

27. R. S. Mulliken, Rev. Mod. Phys., Vol. 14, p. 204, 1942

28. A. D. Walsh, J. Chem. Soc., p. 2266, 1953

29. R. S. Mulliken, Can. J. Chem., Vol. 36, p. 10, 1958

30. K. L. McEwen, J. Chem. Phys., Vol. 32, p. 1801, 1960

31. M. Green and J. W. Linnett, Trans. Faraday Soc., Vol. 57, p. 1, 1961

32. V. N. Soshnikov, Opt. Spectry., Vol. 6, p. 203, 1959

33. V. N. Soshnikov, Opt. Spectry., Vol. 13, p. 500, 1962

34. R. Dickinson and W. Baxter, J. Am. Chem. Soc., Vol. 50, p. 774, 1928

35. H. H. Holmes and F. Daniels, J. Am. Chem. Soc., Vol. 56, p. 630, 1934

36. J. K. Dixon, J. Chem. Phys., Vol. 8, p. 157, 1940

37. W. C. Price and D. M. Simpson, Trans. Faraday Soc., Vol. 37, p. 106, 1941

38. T. C. Hall and F. E. Blacet, J. Chem. Phys., Vol. 20, p. 1745, 1952

39. K. Mori, Science of Light (Tokyo), Vol. 3, p. 62, 1954; Vol. 4, p. 130, 1955

40. L. Harris, G. W. King, W. S. Benedict, and R. W. B. Pearse, J. Chem. Phys., Vol. 8, p. 765, 1940

41. C. C. Petty, The Absorption of NO_2, HNO_2, and DNO_2, Johns Hopkins University, 1953 (Unpublished)

42. D. F. Heath and G. H. Dieke, Absorption of NO_2, 1957 (Unpublished)

43. Iu. P. Raizer, JETP, Vol. 34, p. 331, 1958

44. G. Schott and N. Davidson, J. Am. Chem. Soc., Vol. 80, p. 1841, 1958

45. B. P. Levitt, Trans. Faraday Soc., Vol. 58, p. 1789, 1962